

Pertinent Dirac structure for QCD sum rules of meson-baryon coupling constants

Takumi Doi¹*, Hungchong Kim² and Makoto Oka¹

¹ *Department of Physics, Tokyo Institute of Technology, Tokyo 152-8551, Japan*

² *Institute of Physics and Applied Physics, Yonsei University, Seoul 120-749, Korea*

Abstract

Using general baryon interpolating fields J_B for $B = N, \Xi, \Sigma$, without derivative, we study QCD sum rules for meson-baryon couplings and their dependence on Dirac structures for the two-point correlation function with a meson $i \int d^4x e^{iqx} \langle 0 | T [J_B(x) \bar{J}_B(0)] | \mathcal{M}(p) \rangle$. Three distinct Dirac structures are compared: $i\gamma_5$, $i\gamma_5 \not{p}$, and $\gamma_5 \sigma_{\mu\nu} q^\mu p^\nu$ structures. From the dependence of the OPE on general baryon interpolating fields, we propose criteria for choosing an appropriate Dirac structure for the coupling sum rules. The $\gamma_5 \sigma_{\mu\nu} q^\mu p^\nu$ sum rules satisfy the criteria while the $i\gamma_5$ sum rules beyond the chiral limit do not. For the $i\gamma_5 \not{p}$ sum rules, the large continuum contributions prohibit reliable prediction for the couplings. Thus, the $\gamma_5 \sigma_{\mu\nu} q^\mu p^\nu$ structure seems pertinent for realistic predictions. In the SU(3) limit, we identify the OPE terms responsible for the F/D ratio. We then study the dependence of the ratio on the baryon interpolating fields. We conclude the ratio $F/D \sim 0.6 - 0.8$ for appropriate choice of the interpolating fields.

PACS: 13.75.Gx; 12.38.Lg; 11.55.Hx

Keywords: QCD Sum rules; meson-baryon couplings, SU(3), F/D ratio

Typeset using REVTeX

*E-mail : doi@th.phys.titech.ac.jp

I. INTRODUCTION

In QCD sum rule approaches [1], the two-point correlation function with a pion

$$i \int d^4x e^{iq \cdot x} \langle 0 | T [J_N(x) \bar{J}_N(0)] | \pi(p) \rangle \quad (1)$$

is often used to calculate the πNN coupling [2–8] by facilitating a general external field method developed in Ref. [9]. This correlation function contains three distinct Dirac structures (1) $i\gamma_5$ (PS), (2) $\gamma_5\sigma_{\mu\nu}q^\mu p^\nu$ (T), and (3) $i\gamma_5\not{p}$ (PV), each of which can in principle be used to calculate the coupling. Currently, there is an issue of the Dirac structure dependence of the sum rule results [4,5]. In calculating the coupling, one can construct either the PS sum rules beyond the chiral limit [6,7] or the T sum rules [4,8]. Both sum rules yield the πNN coupling close to its empirical value. On the other hand, the $i\gamma_5\not{p}$ sum rules contain large contributions from the continuum, which therefore do not provide reliable results.

The PS and T sum rules have been extended to calculate the meson-baryon couplings ηNN , $\pi\Xi\Xi$, $\eta\Xi\Xi$, $\pi\Sigma\Sigma$ and $\eta\Sigma\Sigma$ [7,8] by considering the two-point correlation function with a meson,

$$i \int d^4x e^{iq \cdot x} \langle 0 | T [J_B(x) \bar{J}_B(0)] | \mathcal{M}(p) \rangle . \quad (2)$$

Calculation of the couplings from this correlation function is somewhat limited due to the ignorance of meson wave functions when heavier mesons are involved. In the SU(3) limit however, this correlation function can be used to determine the so-called F/D ratio unambiguously because in this limit the OPE can be exactly classified [7,8] according to SU(3) relations for the couplings [10]. The F/D ratio is an important input in making realistic potential models for hyperon-baryon interactions [11,12] as well as in analyzing the hyperon semileptonic data.

At present, there is a clear Dirac structure dependence in the calculation of the F/D ratio using Eq. (2). In particular, we have reported from the PS sum rules $F/D \sim 0.2$ [7] while from T sum rules $F/D \sim 0.78$ [8]. Thus, even though the two sum rules with different Dirac structures were successful in reproducing the empirical πNN coupling, their prediction for the F/D ratio is quite different.

To resolve this issue, additional criteria to choose a proper Dirac structure are needed for reliable predictions on the F/D ratio as well as the meson-baryon couplings. For this purpose, we first note that in Ref. [7,8] the Ioffe current or its SU(3) rotated version has been used to construct sum rules Eq. (2). The Ioffe current however is a specific choice for the nucleon current among infinitely many possibilities. The Ioffe current is often used for the nucleon because it gets large contributions from the chiral breaking parameter $\langle \bar{q}q \rangle$. In addition, direct instantons are believed to play less roles in this current.

Nevertheless, it may be useful to study the dependence of the sum rule results on general baryon currents. Depending on the currents, it is expected that the overlap λ_B between the physical baryon state and the current may be altered but ideally the physical parameters such as meson-baryon couplings remain unchanged. Indeed, from the correlation function Eq. (2), what will actually be determined is the overlap strength multiplied by the coupling of concern. In the SU(3) symmetric limit, all the strengths depend only on the currents. They are determined from the corresponding baryon mass sum rules and all the baryon

masses are the same in the SU(3) limit. Thus, in this limit, the dependence on the currents should be driven by the common overlap strength, which in return provides the coupling independent of the currents. This ideal aspect will be pursued in this work as a criterion for choosing a proper Dirac structure.

An alternative way is to calculate baryon axial charges and convert them into meson-baryon couplings using the Goldberger-Treiman relation. Ref. [13] considered the nucleon correlation function in external axial vector field and constructed a sum rule for $g_A - 1$ using one specific Dirac structure. Recently, a new approach was proposed in Ref. [14] where the axial vector correlation function in a one-nucleon state is considered. Both obtained an excellent agreement for g_A of the nucleon.

This paper is organized as follows. In Section II, we construct meson-baryon coupling sum rules using general baryon currents. A brief discussion on the OPE based on chirality is given in Section III. We then briefly check in Section IV whether the discussion on the continuum threshold [5,8] is still valid when the general baryon currents are used in the sum rules. In Section V, the dependence of the OPE on the baryon currents is studied. We study in the SU(3) limit whether or not the dependence on the currents are mostly contained in the overlap λ_B . This constraint gives us a new criterion to choose an appropriate Dirac structure. In Section VI, we calculate the couplings in the SU(3) limit from the $\gamma_5 \sigma_{\mu\nu} q^\mu p^\nu$ structure. The F/D ratio is identified in terms of the OPE. Conclusions are given in Section VII.

II. CONSTRUCTION OF THE QCD SUM RULES

We use the two-point correlation function with a meson,

$$i \int d^4x e^{iq \cdot x} \langle 0 | T [J_B(x) \bar{J}_B(0)] | \mathcal{M}(p) \rangle \quad (3)$$

where J_B is the baryon current of concern and p is the momentum of meson \mathcal{M} . Meson states π and η , and baryon currents for the proton, Ξ and Σ will be considered in this work.

The proton current is constructed from two u -quarks and one d -quark by assuming that all three quarks are in the s-wave state. In the construction of the current, one up and one down quark are combined into an isoscalar diquark. The other up quark is attached to the diquark so that quantum numbers of the proton are carried by the attached up quark. In this method, there are two possible combinations for the current. The general proton current is a linear combination of the two possibilities mediated by a real parameter t ,

$$J_p(x; t) = 2\epsilon_{abc} [(u_a^T(x) C d_b(x)) \gamma_5 u_c(x) + t (u_a^T(x) C \gamma_5 d_b(x)) u_c(x)] . \quad (4)$$

Here, a, b, c are color indices, T denotes the transpose with respect to the Dirac indices, and C the charge conjugation. The choice $t = -1$ is called the Ioffe current [15]. The currents for Ξ and Σ are obtained from the proton current via SU(3) rotations [16],

$$\begin{aligned} J_\Xi(x; t) &= -2\epsilon_{abc} [(s_a^T(x) C u_b(x)) \gamma_5 s_c(x) + t (s_a^T(x) C \gamma_5 u_b(x)) s_c(x)] , \\ J_\Sigma(x; t) &= 2\epsilon_{abc} [(u_a^T(x) C s_b(x)) \gamma_5 u_c(x) + t (u_a^T(x) C \gamma_5 s_b(x)) u_c(x)] . \end{aligned} \quad (5)$$

When going beyond the soft-meson limit, one can consider three distinct Dirac structures in correlation function in constructing sum rules: $i\gamma_5$ (PS), $\gamma_5 \sigma_{\mu\nu} q^\mu p^\nu$ (T) and $i\gamma_5 \not{p}$ (PV).

For the $i\gamma_5$ structure, the sum rules are constructed at the order $p^2 = m_\pi^2$ [6]. At this order, the terms linear in quark mass (m_q) in the OPE should be included because m_q is the same chiral order with m_π^2 via the Gell-Mann–Oakes–Renner relation,

$$-2m_q\langle\bar{q}q\rangle = m_\pi^2 f_\pi^2. \quad (6)$$

On the other hand, for the T and PV structures, we construct the sum rules at the order $\mathcal{O}(p)$. At this order, the m_q terms should not be included in the OPE. Technical details on the OPE calculation can be found in Refs. [7,8].

In constructing the phenomenological side, we first define $\lambda_B(t)$, the coupling strength between the baryon current $J_B(x;t)$ and the physical baryon field $\psi_B(x)$. Using the pseudoscalar type interaction between the meson and baryons $g_{MB}\bar{\psi}_B i\gamma_5 \psi_B \mathcal{M}$, we obtain the phenomenological side of the correlation function:

$$i\gamma_5 \text{ structure} \quad \text{at the order } \mathcal{O}(p^2) \quad i\gamma_5 p^2 \frac{g_{MB}\lambda_B^2(t)}{(q^2 - m_B^2)^2} + \dots, \quad (7)$$

$$\gamma_5 \sigma_{\mu\nu} q^\mu p^\nu \text{ structure at the order } \mathcal{O}(p) \quad \gamma_5 \sigma_{\mu\nu} q^\mu p^\nu \frac{g_{MB}\lambda_B^2(t)}{(q^2 - m_B^2)^2} + \dots, \quad (8)$$

$$i\gamma_5 \not{p} \text{ structure} \quad \text{at the order } \mathcal{O}(p) \quad -i\gamma_5 \not{p} \frac{g_{MB}\lambda_B^2(t)m_B}{(q^2 - m_B^2)^2} + \dots. \quad (9)$$

The ellipsis denotes contributions from higher resonances as well as a single pole associated with transitions from the ground state to higher resonances. The continuum contributions come from transitions among higher resonances, whose spectral densities are modeled with a step function starting at the threshold S_0 . Matching the OPE side with the phenomenological side and taking Borel transformation¹, we get the sum rules of the form

$$g_{MB}\lambda_B^2(t) \left[1 + A_{MB}(t)M^2 \right] = e^{m_B^2/M^2} \cdot F_{MB}^{\text{OPE}}(M^2; t) \equiv f_{MB}^{\text{OPE}}(M^2; t) \quad (10)$$

where the single pole term in the phenomenological side has been denoted by A_{MB} . Expressions for the OPE $F_{MB}^{\text{OPE}}(M^2; t)$ are given in the Appendix A.

III. CHIRALITY CONSIDERATION

The OPEs given in the Appendix A have an interesting feature to discuss when $t = 1$. Specifically, in the $i\gamma_5$ and $\gamma_5 \sigma_{\mu\nu} q^\mu p^\nu$ sum rules, Wilson coefficients of chiral-odd operators $\langle\bar{q}q\rangle$, $f_{3\pi}$, $\langle\bar{q}q\rangle \left\langle \frac{\alpha_s}{\pi} \mathcal{G}^2 \right\rangle$, and $m_0^2 \langle\bar{q}q\rangle$ are all zero when $t = 1$. Also in the $i\gamma_5 \not{p}$ sum rules, contributions from the chiral-even operators $\langle\bar{q}q\rangle^2$ and $m_0^2 \langle\bar{q}q\rangle^2$ are zero. To understand this feature, it is useful to decompose the correlator according to chirality of the current,

$$J_B \bar{J}_B = J_B^R \bar{J}_B^R + J_B^R \bar{J}_B^L + J_B^L \bar{J}_B^R + J_B^L \bar{J}_B^L. \quad (11)$$

¹Note, we use a single dispersion relation as advocated in Ref. [17,18].

$J_B^L(J_B^R)$ denotes the left-handed (right-handed) component of the current J_B . On the other hand, Eq. (3) can be written

$$i \int d^4x e^{iq \cdot x} \langle 0 | T [J_B(x) \bar{J}_B(0)] | \mathcal{M}(p) \rangle = i\gamma_5 \Pi_{ps} + i\gamma_5 \not{p} \Pi_{pv} + \gamma_5 \sigma_{\mu\nu} q^\mu p^\nu \Pi_T . \quad (12)$$

Thus, it is easy to see that the $i\gamma_5$ and $\gamma_5 \sigma_{\mu\nu}$ structures have nonzero contributions only from the chiral mixing term $J^R \bar{J}^L + J^L \bar{J}^R$, while the chirality conserving term $J^R \bar{J}^R + J^L \bar{J}^L$ contributes only to the $i\gamma_5 \not{p}$ structure.

Now let us classify QCD operators contributing to each Dirac structure. To do that, we suppress for simplicity the color indices and write baryon current as

$$J \sim (q^T C q) \gamma_5 q + t (q^T C \gamma_5 q) q . \quad (13)$$

Here $q = u, d, s$. When $t = 1$, it is straightforward to show that

$$J_R \sim 2(q_R^T C q_R) q_R , \quad (14)$$

$$J_L \sim -2(q_L^T C q_L) q_L . \quad (15)$$

Thus, at this specific t , chirality of all quarks are the same as that of the baryon.

In the $i\gamma_5$ or $\gamma_5 \sigma_{\mu\nu}$ sum rules, we need to consider the products $J^R \bar{J}^L$ and $J^L \bar{J}^R$. In making such products using Eqs. (14) (15), all three quark propagators should break the chirality when they move from the coordinate 0 to x . Hence, it is easy to see that, among chiral-odd operators, terms such as

$$m_q \langle \bar{q}q \rangle^2, \langle \bar{q}q \rangle^3, m_q^2 \langle \bar{q}q \rangle, \dots \quad (16)$$

can contribute to the $i\gamma_5$ or $\gamma_5 \sigma_{\mu\nu}$ correlator, while other chiral-odd operators such as $\langle \bar{q}q \rangle$, $f_{3\pi}$, $\langle \bar{q}q \rangle \langle \frac{\alpha_s}{\pi} \mathcal{G}^2 \rangle$, $m_0^2 \langle \bar{q}q \rangle$ cannot.

On the other hand, in the $i\gamma_5 \not{p}$ structure, the product $J^L \bar{J}^L$ or $J^R \bar{J}^R$ contributes to the sum rule. Among chiral-even operators, an operator such as $\langle \bar{q}q \rangle^2$ cannot be formed in the product $J^L \bar{J}^L$ or $J^R \bar{J}^R$ simply because two quarks with the same chirality cannot be combined into the quark-antiquark pair. Similarly, $m_0^2 \langle \bar{q}q \rangle^2$ can not be formed. This explains the disappearance of such terms in the OPE when $t = 1$.

IV. CRITERION I : SENSITIVITY TO THE CONTINUUM THRESHOLD

We now analyze sum rules of the three different Dirac structures with the general baryon currents, Eqs (4) and (5). As pointed out in Refs. [5,8], sum rule results from the $i\gamma_5 \not{p}$ structure are sensitive to the continuum threshold S_0 and therefore this structure is not reliable. On the other hand, $i\gamma_5$ and $\gamma_5 \sigma_{\mu\nu} q^\mu p^\nu$ structures are insensitive to S_0 . The chirality consideration suggested in Ref. [5] implies that in the $i\gamma_5 \not{p}$ sum rules the large slope and the strong sensitivity to S_0 of the Borel curves can be explained if higher resonances with different parities add up. With this scenario, the higher resonances contributions cancel each other in the $i\gamma_5$ and $\gamma_5 \sigma_{\mu\nu} q^\mu p^\nu$ sum rules therefore explaining the weak sensitivity to S_0 and the small slope of the Borel curves.

Since only the Ioffe current is used in the analysis of Refs. [5,8], let us briefly check if this scenario still works when the general baryon currents are used. As the scenario does not rely on the specific form for the current, what has been claimed in Refs. [5,8] must be valid even with the general baryon currents. To see this, we plot the RHS of Eq. (10) for the πNN coupling from $i\gamma_5$, $\gamma_5\sigma_{\mu\nu}q^\mu p^\nu$ and $i\gamma_5\not{p}$ structures in Figs. 1, 2, 3, respectively. To show the dependence on t , we plot the curves for $t = -1.5, 1.5$ as well as $t = -1.0$ (the Ioffe current). In these plots, we use the standard QCD parameters,

$$\begin{aligned} \langle \bar{q}q \rangle &= -(0.23 \text{ GeV})^3 ; & \left\langle \frac{\alpha_s}{\pi} \mathcal{G}^2 \right\rangle &= (0.33 \text{ GeV})^4 , \\ \delta^2 &= 0.2 \text{ GeV}^2 ; & m_0^2 &= 0.8 \text{ GeV}^2 . \end{aligned} \quad (17)$$

For each t , the thick lines are for the continuum threshold $S_0 = 2.07 \text{ GeV}^2$ corresponding to the Roper resonance, while the thin lines for $S_0 = 2.57 \text{ GeV}^2$. The trend observed here is the same for the other couplings.

In Fig. 3, we observe that the $i\gamma_5\not{p}$ structure is sensitive to the continuum threshold even when the general current is used. The difference by changing the continuum threshold is $\sim 15\%$ at $M^2 = 1 \text{ GeV}^2$. Note also that the slope is relatively large in this case. Since the coupling is determined from the intersection of the best fitting curve with the vertical line at $M^2 = 0$ (see Eq. (10)), the 15% change at $M^2 = 1 \text{ GeV}^2$, when it combined with the large slope, produces huge change in the extracted coupling. In contrast, from Figs. 1 and 2, the $i\gamma_5$ and $\gamma_5\sigma_{\mu\nu}q^\mu p^\nu$ structures are insensitive to S_0 . Also the slopes of the curves are small. This observation is practically independent of the parameter t . At $M^2 = 1 \text{ GeV}^2$, the difference is only 2–3% level. Thus, the analysis in Refs. [5,8] is still valid and the sum rule results from $i\gamma_5\not{p}$ structure should be discarded under this consideration.

V. CRITERION II : THE DEPENDENCE OF THE OPE ON BARYON CURRENTS

Using the sum rules derived in Section II, we discuss the dependence of the OPE on the baryon current (i.e. the dependence on t). For a given t , we linearly fit the RHS of Eq. (10)

$$g_{MB}\lambda_B^2(t) \left[1 + A_{MB}(t)M^2 \right] = f_{MB}^{\text{OPE}}(M^2; t) ,$$

and determine $[g_{MB}\lambda_B^2(t)]_{\text{fitted}}$. Because f_{MB}^{OPE} is quadratic in t , $[g_{MB}\lambda_B^2(t)]_{\text{fitted}}$ is also quadratic. Ideally, the physical parameter g_{MB} should be independent of t if the sum rules are reliable. In other words, t is just a parameter for the current. By changing t , only the coupling strength $\lambda_B^2(t)$ is expected to be affected, but not the physical parameter. This is a constraint to be satisfied when the sum rules are “good.”

To proceed, we take the SU(3) symmetric limit. Then, the strength $\lambda_B(t)$ should be independent of the baryons,

$$\lambda_N(t) = \lambda_\Xi(t) = \lambda_\Sigma(t) , \quad (18)$$

as the baryon mass sum rules are the same in the limit. Furthermore, we have

$$\begin{aligned}
\langle \bar{s}s \rangle &= \langle \bar{q}q \rangle & ; & \quad m_\eta = m_\pi , \\
f_\eta &= f_\pi & ; & \quad f_{3\eta} = f_{3\pi} , \\
m_N &= m_\Xi = m_\Sigma & ; & \quad m_s = m_q .
\end{aligned}
\tag{19}$$

This SU(3) limit is particularly interesting when we select a suitable Dirac structure. Suppose we plot $[g_{MB}\lambda_B^2(t)]_{\text{fitted}}$ in terms of t . If the sum rules are “good”, all g_{MB} should be just constants, independent of t . The functional behavior is driven only by the strength $\lambda_B^2(t)$. The baryon mass sum rules in the SU(3) limit constrain that all $\lambda_B^2(t)$ are *the same* irrespective of the baryons. Therefore, “good” sum rules must give $[g_{MB}\lambda_B^2(t)]_{\text{fitted}}$ which are proportional to each other.

Our constraint should be satisfied when the OPE are exact. But in practice, the full OPE terms $f_{\text{full}}^{\text{OPE}}$ are separated into two groups,

$$f_{\text{full}}^{\text{OPE}} = f_{\text{calc}}^{\text{OPE}} + f_{\text{rest}}^{\text{OPE}} , \tag{20}$$

where $f_{\text{calc}}^{\text{OPE}}$ denotes the calculable OPE, and $f_{\text{rest}}^{\text{OPE}}$ denotes the rest of the full OPE. In this notation, the reliability of sum rule simply means

$$f_{\text{calc}}^{\text{OPE}} \gg f_{\text{rest}}^{\text{OPE}} . \tag{21}$$

The sum rules are “unreliable” if

$$f_{\text{calc}}^{\text{OPE}} \sim f_{\text{rest}}^{\text{OPE}} . \tag{22}$$

In the former case, we expect that $[g_{MB}\lambda_B^2(t)]_{\text{fitted}}$ derived from $f_{\text{calc}}^{\text{OPE}}$ is almost the same as those from $f_{\text{full}}^{\text{OPE}}$ in most region of t . On the other hand, in the latter case, $[g_{MB}\lambda_B^2(t)]_{\text{fitted}}$ derived from $f_{\text{calc}}^{\text{OPE}}$ may be quite different from those obtained from $f_{\text{full}}^{\text{OPE}}$, and our ideal constraint may not be satisfied in most t .

Therefore, the ideal constraint can be used as a new criterion for choosing reliable sum rules. In order to apply this constraint to our sum rules, we again use the standard QCD parameters Eq. (17) and linearly fit $[g_{MB}\lambda_B^2(t)]_{\text{fitted}}$ at each t . In the fitting, the continuum threshold is set to $S_0 = 2.07 \text{ GeV}^2$, corresponding to the Roper resonance, and the Borel window is taken $0.65 \leq M^2 \leq 1.24 \text{ GeV}^2$ as in Refs. [6–8]. In this Borel window, (1) the Borel curve for each coupling is almost linear (see Figs. 1, 2), (2) the contribution from the highest dimensional OPE term is typically 5–15% in the $\gamma_5\sigma_{\mu\nu}q^\mu p^\nu$ sum rules and 20% level in the $i\gamma_5$ sum rules, and (3) the continuum contribution is less than 20% in both structures. It should be noted that because all the couplings are related under SU(3) rotations, we need to take a common Borel window [7,8].

Fig. 4 shows $[g_{MB}\lambda_B^2(t)]_{\text{fitted}}$ as a function of t for the $i\gamma_5$ sum rules. The $\gamma_5\sigma_{\mu\nu}q^\mu p^\nu$ cases are shown in Fig. 5. Interesting features in the $\gamma_5\sigma_{\mu\nu}q^\mu p^\nu$ cases are that (1) all the curves are zero when $t = 1$ and almost zero at $t \sim -0.5$, (2) each extremum of the curves coincides around $t \sim 0.3$. Under the chirality consideration given in Section III, we can easily understand why $[g_{MB}\lambda_B^2(t)]_{\text{fitted}}$ is zero when $t = 1$. From the figure, though not exact, one observes that the curves can be almost overlapped when multiplied by appropriate constants. For example, let us compare the πNN and ηNN curves. When they are positive, the πNN curve lies above the ηNN curve. When they are negative, the situation is reversed. This behavior of the ηNN curve can be reproduced by multiplying an appropriate constant to

the πNN curve. Of course, this claim can not be made when $t \sim -0.5$ because one curve becomes zero while the other does not. Therefore, except around $t \sim -0.5$, the Borel curves satisfy the ideal constraint in most region of t . Such a trend can not be observed from the $i\gamma_5$ sum rules. (see Fig. 4.) Therefore, we claim that the $\gamma_5\sigma_{\mu\nu}q^\mu p^\nu$ sum rules are more appropriate.

To support our claim that the $\gamma_5\sigma_{\mu\nu}q^\mu p^\nu$ sum rules are more suitable than those from the $i\gamma_5$ structure, one more check to do is to see the t -dependence of $\lambda_B^2(t)$ from baryon mass sum rules. In Fig. 6, $\lambda_B^2(t)$ in the SU(3) limit is plotted using chiral-odd nucleon mass sum rule ²:

$$m_B\lambda_B^2(t)e^{-m_B^2/M^2} = \frac{-4}{(2\pi)^4} \left[\frac{\pi^2}{4}(-5 - 2t + 7t^2)\langle\bar{q}q\rangle M^4 E_1(x) + \frac{3}{4}\pi^2(1 - t^2)m_0^2\langle\bar{q}q\rangle M^2 E_0(x) + \frac{\pi^4}{24}(-7 + 2t + 5t^2)\langle\bar{q}q\rangle \left\langle \frac{\alpha_s}{\pi} \mathcal{G}^2 \right\rangle \right], \quad (23)$$

where m_q order terms are neglected and the SU(3) relations are used: $m_N = m_\Xi = m_\Sigma \equiv m_B$; $\lambda_N = \lambda_\Xi = \lambda_\Sigma \equiv \lambda_B$; $\langle\bar{u}u\rangle = \langle\bar{d}d\rangle = \langle\bar{s}s\rangle \equiv \langle\bar{q}q\rangle$. Comparing with Fig. 5, we confirm that the t -dependence of $[g_{\mathcal{M}B}\lambda_B^2(t)]_{\text{fitted}}$ from the $\gamma_5\sigma_{\mu\nu}q^\mu p^\nu$ sum rules can be reproduced from the t -dependence of $\lambda_B^2(t)$.

In the region $-0.5 \lesssim t \lesssim 1$ in Fig. 6, $\lambda_B^2(t)$ is negative, thus not physical. In this region, the sum rules should definitely fail and a reliable prediction for a physical parameter may not be possible. At $t \sim -0.5$ or $t \sim 1$, of course, the OPE is almost zero suggesting that there are cancellations among OPE terms, i.e. the correlation function can not be well saturated by the calculated OPE. Therefore, the optimal current should be chosen away from these points.

VI. THE F/D RATIO FROM THE PSEUDOTENSOR SUM RULES

In this section, we analyze the $\gamma_5\sigma_{\mu\nu}q^\mu p^\nu$ sum rules to determine the F/D ratio. In particular, we investigate the t -dependence of the ratio using the general interpolating fields for the baryons. As already mentioned, mesons and baryons are classified according to SU(3) symmetry, which provides simple relations for the meson-baryon couplings in terms of the two parameters [10]

$$g_{\pi N} \quad \text{and} \quad \alpha = \frac{F}{F + D}. \quad (24)$$

That is,

²Definition of the function $E_n(x \equiv S_0/M^2)$ is given in the Appendix A. The Wilson coefficient of the dimension 7 OPE is different from Ref. [19]. When $t = -1$ (the Ioffe current), however, our Wilson coefficient reduces to that of Ref. [9]. Nevertheless, the dimension 7 condensate contributes to the sum rule only slightly. Thus, this discrepancy is marginal.

$$\begin{aligned}
g_{\eta N} &= \frac{1}{\sqrt{3}}(4\alpha - 1)g_{\pi N} ; & g_{\pi \Xi} &= (2\alpha - 1)g_{\pi N} , \\
g_{\eta \Xi} &= -\frac{1}{\sqrt{3}}(1 + 2\alpha)g_{\pi N} ; & g_{\pi \Sigma} &= 2\alpha g_{\pi N} , \\
g_{\eta \Sigma} &= \frac{2}{\sqrt{3}}(1 - \alpha)g_{\pi N} .
\end{aligned} \tag{25}$$

To see how these relations are reflected in the OPE of the $\gamma_5 \sigma_{\mu\nu} q^\mu p^\nu$ sum rules (see the Appendix A for the OPE), we take the SU(3) symmetric limit to organize them in terms of two terms \mathcal{O}_1 and \mathcal{O}_2 defined as

$$\begin{aligned}
\mathcal{O}_1 \cdot e^{-m_B^2/M^2} &\equiv \frac{1}{96\pi^2 f_\pi}(-2 + 4t - 2t^2)\langle \bar{q}q \rangle M^4 E_0(x) - \frac{f_\pi}{3}(-1 + t^2)\langle \bar{q}q \rangle M^2 \\
&\quad - \frac{1}{54}f_\pi \delta^2 7(-1 + t^2)\langle \bar{q}q \rangle + \frac{1}{72 \cdot 12 f_\pi}(-1 + 2t - t^2)\langle \bar{q}q \rangle \left\langle \frac{\alpha_s}{\pi} \mathcal{G}^2 \right\rangle \\
&\quad + \frac{f_\pi}{72}7(-1 + t^2)m_0^2 \langle \bar{q}q \rangle ,
\end{aligned} \tag{26}$$

$$\begin{aligned}
\mathcal{O}_2 \cdot e^{-m_B^2/M^2} &\equiv \frac{1}{96\pi^2 f_\pi}12(1 - t^2)\langle \bar{q}q \rangle M^4 E_0(x) + \frac{2f_\pi}{3}(t - t^2)\langle \bar{q}q \rangle M^2 \\
&\quad - \frac{1}{27}f_\pi \delta^2 (3 - 13t + 10t^2)\langle \bar{q}q \rangle + \frac{1}{48 f_\pi}(1 - t^2)\langle \bar{q}q \rangle \left\langle \frac{\alpha_s}{\pi} \mathcal{G}^2 \right\rangle \\
&\quad + \frac{f_\pi}{36}(1 - 3t + 2t^2)m_0^2 \langle \bar{q}q \rangle .
\end{aligned} \tag{27}$$

Specifically, we have

$$\begin{aligned}
g_{\pi N} \cdot \lambda_N^2(1 + A_{\pi N}M^2) &= \mathcal{O}_1 + \mathcal{O}_2 , \\
\sqrt{3}g_{\eta N} \cdot \lambda_N^2(1 + A_{\eta N}M^2) &= -\mathcal{O}_1 + \mathcal{O}_2 , \\
g_{\pi \Xi} \cdot \lambda_N^2(1 + A_{\pi \Xi}M^2) &= -\mathcal{O}_1 , \\
\sqrt{3}g_{\eta \Xi} \cdot \lambda_N^2(1 + A_{\eta \Xi}M^2) &= -\mathcal{O}_1 - 2\mathcal{O}_2 , \\
g_{\pi \Sigma} \cdot \lambda_N^2(1 + A_{\pi \Sigma}M^2) &= \mathcal{O}_2 , \\
\sqrt{3}g_{\eta \Sigma} \cdot \lambda_N^2(1 + A_{\eta \Sigma}M^2) &= 2\mathcal{O}_1 + \mathcal{O}_2 .
\end{aligned} \tag{28}$$

Note that another SU(3) relation $\lambda_N = \lambda_\Xi = \lambda_\Sigma$ has been used in writing these equations. Neglecting the unknown single pole term $A_{\mathcal{M}B}$, we identify the F/D ratio in terms of the OPE,

$$2\alpha \sim \frac{\mathcal{O}_2}{\mathcal{O}_1 + \mathcal{O}_2} \quad \longrightarrow \quad F/D \sim \frac{\mathcal{O}_2}{2\mathcal{O}_1 + \mathcal{O}_2} . \tag{29}$$

This is an obvious consequence of using the baryon currents constructed according to the SU(3) symmetry. Hence, it provides the consistency of our sum rules with the SU(3) relations for the couplings.

To determine the F/D ratio, however, the unknown single pole term A_{MB} should be taken into account. For that purpose, we linearly fit the RHS of Eq. (28) and determine $[g_{MB}\lambda_B^2(t)]_{\text{fitted}}$ for a given t . Once two of $[g_{MB}\lambda_B^2(t)]_{\text{fitted}}$ are determined, their ratio can be converted to yield the F/D ratio according to Eq. (25).

In Fig. 7, the F/D ratio is plotted as a function of $\cos\theta$. Here, to investigate the whole range of $-\infty \leq t \leq +\infty$, we introduce a new parameter θ defined as

$$\tan\theta = t. \quad (30)$$

Thus, the range $0 \leq t \leq +\infty$ corresponds to $0 \leq \theta \leq \pi/2$ while the range $-\infty \leq t \leq 0$ spans $\pi/2 \leq \theta \leq \pi$. In Fig. 7, circles are obtained from the Borel window $0.65 \leq M^2 \leq 1.24 \text{ GeV}^2$ with the continuum threshold $S_0 = 2.07 \text{ GeV}^2$. To see the sensitivity to this choice, we also calculate the ratio using (1) $0.65 \leq M^2 \leq 1.24 \text{ GeV}^2$, $S_0 = 2.57 \text{ GeV}^2$ (triangles), (2) $0.90 \leq M^2 \leq 1.50 \text{ GeV}^2$, $S_0 = 2.07 \text{ GeV}^2$ (squares). We see that the F/D ratio is insensitive to the continuum threshold, agreeing with the discussion in Section IV. Also, the calculated F/D ratio is relatively insensitive to the choice of the Borel window. The peak around $t \sim -0.5$ ($\cos\theta \sim -0.9$) can be understood from Fig. 5. Most curves are zero around this t but not simultaneously. The F/D ratio is basically obtained by taking a ratio of any two curves but the ratio of the two curves around $t \sim -0.5$ ($\cos\theta \sim -0.9$) is not well-behaved. On the other hand, at $t = 1$ ($\cos\theta = 1/\sqrt{2}$), the F/D ratio does not diverge because all curves for the couplings in Fig. 5 go to zero linearly in $(t - 1)$.

The strong sensitivity of the F/D ratio to t within the region $-0.5 \lesssim t \lesssim 1$ ($\cos\theta \lesssim -0.9$, or $0.7 \lesssim \cos\theta$) is unrealistic because first of all, absolute total value of the OPE in each coupling is very small in this region. The convergence of the OPE may not be sufficient enough. Secondly, the strength λ_N^2 as can be seen from Fig. 6 is negative, thus not physical. Therefore, a reasonable value for the F/D ratio should be obtained away from this region. We moderately take the realistic region as (1) $t \lesssim -0.8$ ($-0.78 \lesssim \cos\theta$) and (2) $1.3 \lesssim t$ ($\cos\theta \lesssim 0.61$). The former constraint gives us the maximum value of $F/D \sim 0.84$, and the latter constraint gives us the minimum value of $F/D \sim 0.63$. Therefore, we conclude $F/D \sim 0.6 - 0.8$. This range includes the value from the SU(6) quark model ($F/D = 2/3$), and is slightly higher than that extracted from semi-leptonic decay rates of hyperons ($F/D \sim 0.57$) [20]. It is often argued that the choice of $t = -1$ (the Ioffe current) is optimal because the instanton effect [21] and the continuum contribution [19] is small, and the chiral breaking effects are maximized. If we choose $t \sim -1$, our estimate becomes $F/D \sim 0.76 - 0.81$, that is somewhat larger than the SU(6) value.

As a comparison, let us briefly consider the $i\gamma_5$ structure case. In this case too, we can classify the OPE of the Appendix A 1 according to Eq. (25) and identify the terms responsible for the F/D ratio. By taking similar steps as T sum rules, we determine the F/D ratio. Fig. 8 shows the F/D ratio as a function of $\cos\theta$. Compared with Fig. 7, the F/D ratio is very sensitive to t . As discussed in Section V, $f_{\text{rest}}^{\text{OPE}}$ may cause this huge t -dependence. Another possibility is due to the large contribution from direct instanton in the pseudoscalar channel. The direct instanton effect is believed to cause large OZI breaking in η and η' . To confirm it, it will be necessary to include the direct instanton effect in this pseudoscalar channel. Nevertheless, the correlation function Eq. (3) is often used in literature to calculate various couplings and our study suggests that one has to be careful in choosing a Dirac structure in that correlation function.

VII. CONCLUSIONS

In this work, we calculated the correlation function Eq. (3) for the vertices, πNN , ηNN , $\pi\Xi\Xi$, $\eta\Xi\Xi$, $\pi\Sigma\Sigma$, and $\eta\Sigma\Sigma$, using QCD sum rules. In the construction of sum rules, we used general baryon currents with no derivative instead of the Ioffe current, which enables us to discuss the dependence of sum rule results on currents. We proposed a new criterion to choose a pertinent Dirac structure by studying the dependence of the correlation function on the baryon currents. Specifically, it is imposed that a physical parameter is ideally independent of a chosen current. In checking this constraint, the SU(3) symmetric limit is quite useful as it provides simple relations among the couplings. It is found that the $\gamma_5\sigma_{\mu\nu}q^\mu p^\nu$ structure satisfies the ideal constraint relatively well, which moderately restricts the F/D ratio within the range, $F/D \sim 0.6 - 0.8$. However, the $i\gamma_5$ sum rules beyond the chiral limit do not satisfy the constraint, which provides a large window for the value of the F/D ratio depending on currents.

In the present study, we considered only the SU(3) limit of the meson-baryon couplings. In fact, the OPE for the $\gamma_5\sigma_{\mu\nu}q^\mu p^\nu$ structure given in the Appendix A 2 contain effects of SU(3) breaking partially as $m_N \neq m_\Xi \neq m_\Sigma$, $\lambda_N \neq \lambda_\Xi \neq \lambda_\Sigma$, $\langle\bar{q}q\rangle \neq \langle\bar{s}s\rangle$ and $f_\pi \neq f_\eta$. If we include these differences, obtained coupling constants break the SU(3) symmetry accordingly. We, however, do not quantify this because other sources of SU(3) breaking are expected. Especially, the large strange quark mass (m_s) may cause non-negligible SU(3) breaking effects. So far, the OPE for the $\gamma_5\sigma_{\mu\nu}q^\mu p^\nu$ structure is truncated to $\mathcal{O}(p)$ so that it is consistent with the chiral expansion, while effects of m_s can only be included at $\mathcal{O}(p^2)$. In order to quantify SU(3) breaking effects on the meson-baryon couplings, it will be necessary to include $\mathcal{O}(p^2)$ contribution. The present formulation may give a solid starting point for such analyses in future.

ACKNOWLEDGMENTS

This work was supported in part by the Grant-in-Aid for scientific research (C) (2) 11640261 of the Ministry of Education, Science, Sports and Culture of Japan. H. Kim was supported by the Brain Korea 21 project. We would like to thank Prof. S.H. Lee for useful discussions.

APPENDIX A: COUPLING SUM RULES FROM THE PS, T, PV STRUCTURE

Coupling sum rules for πNN , ηNN , $\pi\Xi\Xi$, $\eta\Xi\Xi$, $\pi\Sigma\Sigma$, and $\eta\Sigma\Sigma$ are presented here. For the η couplings, $\eta - \eta'$ mixing is not introduced because our analysis in this paper is within SU(3). In the OPE side, the quark-gluon mixed condensate is parametrized as $\langle\bar{q}_i g_s \sigma \cdot \mathcal{G} q_i\rangle \equiv m_0^2 \langle\bar{q}_i q_i\rangle$ where $q_i = u, d, s$ -quark. Also, we take the isospin symmetric limit, $\langle\bar{u}u\rangle = \langle\bar{d}d\rangle \equiv \langle\bar{q}q\rangle$ and $m_u = m_d \equiv m_q$. The continuum contribution is denoted by the factor, $E_n(x \equiv S_0/M^2) = 1 - (1 + x + \dots + x^n/n!)e^{-x}$ where S_0 is the continuum threshold.

1. Coupling sum rules from the $i\gamma_5$ structure

Here we present the $i\gamma_5$ sum rules up to dimension 8 constructed at the order $p^2 = m_\pi^2$. $A_{\mathcal{M}B}^{\text{PS}}$ denotes the unknown single-pole term coming from transitions between the ground state baryon and higher resonance states.

$$\begin{aligned}
& g_{\pi N} m_\pi^2 \lambda_N^2 (1 + A_{\pi N}^{\text{PS}} M^2) e^{-m_N^2/M^2} \\
&= -\frac{m_\pi^2}{48\pi^2 f_\pi} (-5 - 2t + 7t^2) \langle \bar{q}q \rangle M^4 E_0(x) + \frac{3f_{3\pi} m_\pi^2}{16\sqrt{2}\pi^2} (-1 + 2t - t^2) M^4 E_0(x) \\
&\quad - \frac{1}{2f_\pi} (-5 - 2t - t^2) m_q \langle \bar{q}q \rangle^2 M^2 - \frac{m_\pi^2}{288f_\pi} (-7 + 2t + 5t^2) \langle \bar{q}q \rangle \left\langle \frac{\alpha_s}{\pi} \mathcal{G}^2 \right\rangle \\
&\quad - \frac{1}{12f_\pi} (-7 - 6t - 7t^2) m_q m_0^2 \langle \bar{q}q \rangle^2
\end{aligned}$$

$$\begin{aligned}
& \sqrt{3} g_{\eta N} m_\eta^2 \lambda_N^2 (1 + A_{\eta N}^{\text{PS}} M^2) e^{-m_N^2/M^2} \\
&= -\frac{m_\eta^2}{48\pi^2 f_\eta} (-7 + 2t + 5t^2) \langle \bar{q}q \rangle M^4 E_0(x) + \frac{3f_{3\eta} m_\eta^2}{16\sqrt{2}\pi^2} (1 - 2t + t^2) M^4 E_0(x) \\
&\quad - \frac{1}{2f_\eta} (-7 - 14t - 3t^2) m_q \langle \bar{q}q \rangle^2 M^2 - \frac{m_\eta^2}{288f_\eta} (-5 - 2t + 7t^2) \langle \bar{q}q \rangle \left\langle \frac{\alpha_s}{\pi} \mathcal{G}^2 \right\rangle \\
&\quad - \frac{1}{12f_\eta} (-5 - 2t - 5t^2) m_q m_0^2 \langle \bar{q}q \rangle^2
\end{aligned}$$

$$\begin{aligned}
& g_{\pi \Xi} m_\pi^2 \lambda_\Xi^2 (1 + A_{\pi \Xi}^{\text{PS}} M^2) e^{-m_\Xi^2/M^2} \\
&= -\frac{m_\pi^2}{48\pi^2 f_\pi} (-1 + 2t - t^2) \langle \bar{q}q \rangle M^4 E_0(x) + \frac{3f_{3\pi} m_\pi^2}{16\sqrt{2}\pi^2} (1 - 2t + t^2) M^4 E_0(x) \\
&\quad - \frac{1}{2f_\pi} (-1 - 6t - t^2) m_s \langle \bar{q}q \rangle \langle \bar{s}s \rangle M^2 - \frac{m_\pi^2}{288f_\pi} (1 - 2t + t^2) \langle \bar{q}q \rangle \left\langle \frac{\alpha_s}{\pi} \mathcal{G}^2 \right\rangle \\
&\quad - \frac{1}{12f_\pi} (1 + 2t + t^2) m_s m_0^2 \langle \bar{q}q \rangle \langle \bar{s}s \rangle
\end{aligned}$$

$$\begin{aligned}
& \sqrt{3} g_{\eta \Xi} m_\eta^2 \lambda_\Xi^2 (1 + A_{\eta \Xi}^{\text{PS}} M^2) e^{-m_\Xi^2/M^2} \\
&= -\frac{m_\eta^2}{48\pi^2 f_\eta} [(-1 + 2t - t^2) \langle \bar{q}q \rangle + 12(1 - t^2) \langle \bar{s}s \rangle] M^4 E_0(x) + \frac{3f_{3\eta} m_\eta^2}{16\sqrt{2}\pi^2} (1 - 2t + t^2) M^4 E_0(x) \\
&\quad - \frac{1}{2f_\eta} [-(1 + 6t + t^2) m_s \langle \bar{q}q \rangle + 2(3 + 4t + t^2) (m_q \langle \bar{q}q \rangle + m_s \langle \bar{s}s \rangle)] \langle \bar{s}s \rangle M^2 \\
&\quad - \frac{m_\eta^2}{288f_\eta} [(1 - 2t + t^2) \langle \bar{q}q \rangle + 12(1 - t^2) \langle \bar{s}s \rangle] \left\langle \frac{\alpha_s}{\pi} \mathcal{G}^2 \right\rangle \\
&\quad - \frac{1}{12f_\eta} [(1 + 2t + t^2) m_s \langle \bar{q}q \rangle + 2(3 + 2t + 3t^2) (m_q \langle \bar{s}s \rangle + m_s \langle \bar{q}q \rangle)] m_0^2 \langle \bar{s}s \rangle
\end{aligned}$$

$$\begin{aligned}
& g_{\pi \Sigma} m_\pi^2 \lambda_\Sigma^2 (1 + A_{\pi \Sigma}^{\text{PS}} M^2) e^{-m_\Sigma^2/M^2} \\
&= -\frac{m_\pi^2}{48\pi^2 f_\pi} (-6 + 6t^2) \langle \bar{q}q \rangle M^4 E_0(x) - \frac{1}{2f_\pi} (-3 - 4t - t^2) (m_q \langle \bar{q}q \rangle + m_s \langle \bar{s}s \rangle) \langle \bar{q}q \rangle M^2
\end{aligned}$$

$$\begin{aligned}
& -\frac{m_\pi^2}{288f_\pi}(-6+6t^2)\langle\bar{q}q\rangle\left\langle\frac{\alpha_s}{\pi}\mathcal{G}^2\right\rangle-\frac{1}{12f_\pi}(-3-2t-3t^2)(m_q\langle\bar{s}s\rangle+m_s\langle\bar{q}q\rangle)m_0^2\langle\bar{q}q\rangle \\
& \sqrt{3}g_{\eta\Sigma}m_\eta^2\lambda_\Sigma^2(1+A_{\eta\Sigma}^{\text{PS}}M^2)e^{-m_\Sigma^2/M^2} \\
& =-\frac{m_\eta^2}{48\pi^2f_\eta}[-6(1-t^2)\langle\bar{q}q\rangle+2(1-2t+t^2)\langle\bar{s}s\rangle]M^4E_0(x)+\frac{3f_{3\eta}m_\eta^2}{16\sqrt{2}\pi^2}(-2+4t-2t^2)M^4E_0(x) \\
& -\frac{1}{2f_\eta}[2(1+6t+t^2)m_q\langle\bar{s}s\rangle-(3+4t+t^2)(m_q\langle\bar{q}q\rangle+m_s\langle\bar{s}s\rangle)]\langle\bar{q}q\rangle M^2 \\
& -\frac{m_\eta^2}{288f_\eta}[-6(1-t^2)\langle\bar{q}q\rangle+2(-1+2t-t^2)\langle\bar{s}s\rangle]\left\langle\frac{\alpha_s}{\pi}\mathcal{G}^2\right\rangle \\
& -\frac{1}{12f_\eta}[-2(1+2t+t^2)m_q\langle\bar{s}s\rangle-(3+2t+3t^2)(m_q\langle\bar{s}s\rangle+m_s\langle\bar{q}q\rangle)]m_0^2\langle\bar{q}q\rangle \tag{A1}
\end{aligned}$$

2. Coupling sum rules from the $\gamma_5\sigma_{\mu\nu}q^\mu p^\nu$ structure

The $\gamma_5\sigma_{\mu\nu}q^\mu p^\nu$ sum rules up to dimension 7 are the following. Again, $A_{\mathcal{M}B}^T$ denotes the unknown single-pole term contribution.

$$\begin{aligned}
& g_{\pi N}\lambda_N^2(1+A_{\pi N}^T M^2)e^{-m_N^2/M^2} \\
& =\frac{1}{96\pi^2f_\pi}(10+4t-14t^2)\langle\bar{q}q\rangle M^4E_0(x)-\frac{f_\pi}{3}(-1-2t+3t^2)\langle\bar{q}q\rangle M^2 \\
& -\frac{1}{54}f_\pi\delta^2(-1-26t+27t^2)\langle\bar{q}q\rangle+\frac{1}{72\cdot 12f_\pi}(17+2t-19t^2)\langle\bar{q}q\rangle\left\langle\frac{\alpha_s}{\pi}\mathcal{G}^2\right\rangle \\
& +\frac{f_\pi}{72}(-5-6t+11t^2)m_0^2\langle\bar{q}q\rangle
\end{aligned}$$

$$\begin{aligned}
& \sqrt{3}g_{\eta N}\lambda_N^2(1+A_{\eta N}^T M^2)e^{-m_N^2/M^2} \\
& =\frac{1}{96\pi^2f_\eta}(14-4t-10t^2)\langle\bar{q}q\rangle M^4E_0(x)-\frac{f_\eta}{3}(1-2t+t^2)\langle\bar{q}q\rangle M^2 \\
& -\frac{1}{54}f_\eta\delta^2(13-26t+13t^2)\langle\bar{q}q\rangle+\frac{1}{72\cdot 12f_\eta}(19-2t-17t^2)\langle\bar{q}q\rangle\left\langle\frac{\alpha_s}{\pi}\mathcal{G}^2\right\rangle \\
& +\frac{f_\eta}{72}(9-6t-3t^2)m_0^2\langle\bar{q}q\rangle
\end{aligned}$$

$$\begin{aligned}
& g_{\pi\Xi}\lambda_\Xi^2(1+A_{\pi\Xi}^T M^2)e^{-m_\Xi^2/M^2} \\
& =\frac{1}{96\pi^2f_\pi}(2-4t+2t^2)\langle\bar{q}q\rangle M^4E_0(x)-\frac{f_\pi}{3}(1-t^2)\langle\bar{s}s\rangle M^2 \\
& -\frac{1}{54}f_\pi\delta^2(7-7t^2)\langle\bar{s}s\rangle+\frac{1}{72\cdot 12f_\pi}(1-2t+t^2)\langle\bar{q}q\rangle\left\langle\frac{\alpha_s}{\pi}\mathcal{G}^2\right\rangle \\
& +\frac{f_\pi}{72}(7-7t^2)m_0^2\langle\bar{s}s\rangle
\end{aligned}$$

$$\sqrt{3}g_{\eta\Xi}\lambda_\Xi^2(1+A_{\eta\Xi}^T M^2)e^{-m_\Xi^2/M^2}$$

$$\begin{aligned}
&= \frac{1}{96\pi^2 f_\eta} \left[(2 - 4t + 2t^2)\langle \bar{q}q \rangle + 24(-1 + t^2)\langle \bar{s}s \rangle \right] M^4 E_0(x) \\
&\quad - \frac{f_\eta}{3} \left[(-2 + 4t - 2t^2)\langle \bar{q}q \rangle + 3(1 - t^2)\langle \bar{s}s \rangle \right] M^2 \\
&\quad - \frac{1}{54} f_\eta \delta^2 \left[26(-1 + 2t - t^2)\langle \bar{q}q \rangle + 21(1 - t^2)\langle \bar{s}s \rangle \right] \\
&\quad + \frac{1}{72 \cdot 12f_\eta} \left[(1 - 2t + t^2)\langle \bar{q}q \rangle + 36(-1 + t^2)\langle \bar{s}s \rangle \right] \left\langle \frac{\alpha_s}{\pi} \mathcal{G}^2 \right\rangle \\
&\quad + \frac{f_\eta}{72} \left[6(-1 + 2t - t^2)\langle \bar{q}q \rangle + 9(1 - t^2)\langle \bar{s}s \rangle \right] m_0^2 \\
&g_{\pi\Sigma} \lambda_\Sigma^2 (1 + A_{\pi\Sigma}^\top M^2) e^{-m_\Sigma^2/M^2} \\
&= \frac{1}{96\pi^2 f_\pi} 12(1 - t^2)\langle \bar{q}q \rangle M^4 E_0(x) - \frac{f_\pi}{3} \left[(-1 + t^2)\langle \bar{q}q \rangle + (1 - 2t + t^2)\langle \bar{s}s \rangle \right] M^2 \\
&\quad - \frac{1}{54} f_\pi \delta^2 \left[7(-1 + t^2)\langle \bar{q}q \rangle + 13(1 - 2t + t^2)\langle \bar{s}s \rangle \right] + \frac{1}{72 \cdot 12f_\pi} 18(1 - t^2)\langle \bar{q}q \rangle \left\langle \frac{\alpha_s}{\pi} \mathcal{G}^2 \right\rangle \\
&\quad + \frac{f_\pi}{72} \left[(-1 + t^2)\langle \bar{q}q \rangle + 3(1 - 2t + t^2)\langle \bar{s}s \rangle \right] m_0^2 \\
&\sqrt{3} g_{\eta\Sigma} \lambda_\Sigma^2 (1 + A_{\eta\Sigma}^\top M^2) e^{-m_\Sigma^2/M^2} \\
&= \frac{1}{96\pi^2 f_\eta} \left[12(1 - t^2)\langle \bar{q}q \rangle + 4(-1 + 2t - t^2)\langle \bar{s}s \rangle \right] M^4 E_0(x) \\
&\quad - \frac{f_\eta}{3} \left[3(-1 + t^2)\langle \bar{q}q \rangle + (1 - 2t + t^2)\langle \bar{s}s \rangle \right] M^2 \\
&\quad - \frac{1}{54} f_\eta \delta^2 \left[21(-1 + t^2)\langle \bar{q}q \rangle + 13(1 - 2t + t^2)\langle \bar{s}s \rangle \right] \\
&\quad + \frac{1}{72 \cdot 12f_\eta} \left[18(1 - t^2)\langle \bar{q}q \rangle + 2(-1 + 2t - t^2)\langle \bar{s}s \rangle \right] \left\langle \frac{\alpha_s}{\pi} \mathcal{G}^2 \right\rangle \\
&\quad + \frac{f_\eta}{72} \left[15(-1 + t^2)\langle \bar{q}q \rangle + 3(1 - 2t + t^2)\langle \bar{s}s \rangle \right] m_0^2 \tag{A2}
\end{aligned}$$

3. Coupling sum rules from the $i\gamma_5\not{p}$ structure

The $i\gamma_5\not{p}$ sum rules up to dimension 7 are presented here.

$$\begin{aligned}
&g_{\pi N} m_N \lambda_N^2 (1 + A_{\pi N}^{\text{PV}} M^2) e^{-m_N^2/M^2} \\
&= \frac{f_\pi}{24\pi^2} (10 + 8t + 10t^2) M^6 E_1(x) - \frac{f_\pi \delta^2}{48\pi^2} (-20 - 16t - 20t^2) M^4 E_0(x) \\
&\quad + \frac{f_\pi}{72} \left\langle \frac{\alpha_s}{\pi} \mathcal{G}^2 \right\rangle (5 + 4t + 5t^2) M^2 + \frac{1}{18f_\pi} \langle \bar{q}q \rangle^2 (-1 - 2t + 3t^2) M^2 \\
&\quad + \frac{f_\pi \delta^2}{36 \cdot 18} \left\langle \frac{\alpha_s}{\pi} \mathcal{G}^2 \right\rangle (-4 - 2t - 4t^2) + \frac{1}{432f_\pi} m_0^2 \langle \bar{q}q \rangle^2 (-5 - 6t + 11t^2) \\
&\sqrt{3} g_{\eta N} m_N \lambda_N^2 (1 + A_{\eta N}^{\text{PV}} M^2) e^{-m_N^2/M^2}
\end{aligned}$$

$$\begin{aligned}
&= \frac{f_\eta}{24\pi^2}(8 + 8t + 8t^2)M^6 E_1(x) - \frac{f_\eta\delta^2}{48\pi^2}(-22 - 4t - 22t^2)M^4 E_0(x) \\
&\quad + \frac{f_\eta}{72} \left\langle \frac{\alpha_s}{\pi} \mathcal{G}^2 \right\rangle (5 + 2t + 5t^2)M^2 + \frac{1}{18f_\eta} \langle \bar{q}q \rangle^2 (1 - 2t + t^2)M^2 \\
&\quad + \frac{f_\eta\delta^2}{36 \cdot 18} \left\langle \frac{\alpha_s}{\pi} \mathcal{G}^2 \right\rangle (-10 - 4t - 10t^2) + \frac{1}{432f_\eta} m_0^2 \langle \bar{q}q \rangle^2 (9 - 6t - 3t^2)
\end{aligned}$$

$$\begin{aligned}
&g_{\pi\Xi} m_\Xi \lambda_\Xi^2 (1 + A_{\pi\Xi}^{\text{PV}} M^2) e^{-m_\Xi^2/M^2} \\
&= \frac{f_\pi}{24\pi^2}(-1 - t^2)M^6 E_1(x) - \frac{f_\pi\delta^2}{48\pi^2}(-1 + 6t - t^2)M^4 E_0(x) \\
&\quad + \frac{f_\pi}{72} \left\langle \frac{\alpha_s}{\pi} \mathcal{G}^2 \right\rangle (-t)M^2 + \frac{1}{18f_\pi} \langle \bar{q}q \rangle \langle \bar{s}s \rangle (1 - t^2)M^2 \\
&\quad + \frac{f_\pi\delta^2}{36 \cdot 18} \left\langle \frac{\alpha_s}{\pi} \mathcal{G}^2 \right\rangle (-3 - t - 3t^2) + \frac{1}{432f_\pi} m_0^2 \langle \bar{q}q \rangle \langle \bar{s}s \rangle (7 - 7t^2)
\end{aligned}$$

$$\begin{aligned}
&\sqrt{3}g_{\eta\Xi} m_\Xi \lambda_\Xi^2 (1 + A_{\eta\Xi}^{\text{PV}} M^2) e^{-m_\Xi^2/M^2} \\
&= \frac{f_\eta}{24\pi^2}(-19 - 16t - 19t^2)M^6 E_1(x) - \frac{f_\eta\delta^2}{48\pi^2}(41 + 26t + 41t^2)M^4 E_0(x) \\
&\quad + \frac{f_\eta}{72} \left\langle \frac{\alpha_s}{\pi} \mathcal{G}^2 \right\rangle (-10 - 7t - 10t^2)M^2 + \frac{1}{18f_\eta} \left[(3 - 3t^2) \langle \bar{q}q \rangle + (-2 + 4t - 2t^2) \langle \bar{s}s \rangle \right] \langle \bar{s}s \rangle M^2 \\
&\quad + \frac{f_\eta\delta^2}{36 \cdot 18} \left\langle \frac{\alpha_s}{\pi} \mathcal{G}^2 \right\rangle (11 + 5t + 11t^2) + \frac{1}{432f_\eta} \left[9(1 - t^2) \langle \bar{q}q \rangle + 6(-1 + 2t - t^2) \langle \bar{s}s \rangle \right] m_0^2 \langle \bar{s}s \rangle
\end{aligned}$$

$$\begin{aligned}
&g_{\pi\Sigma} m_\Sigma \lambda_\Sigma^2 (1 + A_{\pi\Sigma}^{\text{PV}} M^2) e^{-m_\Sigma^2/M^2} \\
&= \frac{f_\pi}{24\pi^2}(9 + 8t + 9t^2)M^6 E_1(x) - \frac{f_\pi\delta^2}{48\pi^2}(-21 - 10t - 21t^2)M^4 E_0(x) \\
&\quad + \frac{f_\pi}{72} \left\langle \frac{\alpha_s}{\pi} \mathcal{G}^2 \right\rangle (5 + 3t + 5t^2)M^2 + \frac{1}{18f_\pi} \left[(1 - 2t + t^2) \langle \bar{q}q \rangle + (-1 + t^2) \langle \bar{s}s \rangle \right] \langle \bar{q}q \rangle M^2 \\
&\quad + \frac{f_\pi\delta^2}{36 \cdot 18} \left\langle \frac{\alpha_s}{\pi} \mathcal{G}^2 \right\rangle (-7 - 3t - 7t^2) + \frac{1}{432f_\pi} \left[-3(-1 + 2t - t^2) \langle \bar{q}q \rangle - (1 - t^2) \langle \bar{s}s \rangle \right] m_0^2 \langle \bar{q}q \rangle
\end{aligned}$$

$$\begin{aligned}
&\sqrt{3}g_{\eta\Sigma} m_\Sigma \lambda_\Sigma^2 (1 + A_{\eta\Sigma}^{\text{PV}} M^2) e^{-m_\Sigma^2/M^2} \\
&= \frac{f_\eta}{24\pi^2}(11 + 8t + 11t^2)M^6 E_1(x) - \frac{f_\eta\delta^2}{48\pi^2}(-19 - 22t - 19t^2)M^4 E_0(x) \\
&\quad + \frac{f_\eta}{72} \left\langle \frac{\alpha_s}{\pi} \mathcal{G}^2 \right\rangle (5 + 5t + 5t^2)M^2 + \frac{1}{18f_\eta} \left[(1 - 2t + t^2) \langle \bar{q}q \rangle - 3(1 - t^2) \langle \bar{s}s \rangle \right] \langle \bar{q}q \rangle M^2 \\
&\quad + \frac{f_\eta\delta^2}{36 \cdot 18} \left\langle \frac{\alpha_s}{\pi} \mathcal{G}^2 \right\rangle (-1 - t - t^2) + \frac{1}{432f_\eta} \left[-3(-1 + 2t - t^2) \langle \bar{q}q \rangle - 15(1 - t^2) \langle \bar{s}s \rangle \right] m_0^2 \langle \bar{q}q \rangle \quad (\text{A3})
\end{aligned}$$

REFERENCES

- [1] M.A. Shifman, A.I. Vainshtein, and V.I. Zakharov, Nucl. Phys. **B 147** (1979) 385, 448.
- [2] H. Shiomi and T. Hatsuda, Nucl. Phys. **A 594** (1995) 294.
- [3] M. C. Birse and B. Krippa, Phys. Lett. B **373** (1996) 9; Phys. Rev. C **54** (1996) 3240.
- [4] H. Kim, S. H. Lee and M. Oka, Phys. Lett. B **453** (1999) 199.
- [5] H. Kim, S. H. Lee and M. Oka, Phys. Rev. D **60** (1999) 034007.
- [6] H. Kim, Eur. Phys. Jour. A7,(2000), 121.
- [7] H. Kim, T. Doi, M. Oka and S. H. Lee, Nucl. Phys. **A662** (2000) 371.
- [8] H. Kim, T. Doi, M. Oka and S. H. Lee, Nucl. Phys. **A678** (2000) 295.;nucl-th/0002011.
- [9] B. L. Ioffe and A. V. Smilga, Nucl. Phys. **B232** (1984) 109.
- [10] J. J. de Swart, Rev. Mod. Phys. **35** (1963) 916.; **37** (1965) 326 (E).
- [11] V. G. J. Stoks and Th. A. Rijken, Phys. Rev. C **59** (1999) 3009.
- [12] Th. A. Rijken, V. G. J. Stoks and Y. Yamamoto, Phys. Rev. C **59** (1999) 21.
- [13] V. M. Belyaev and Ya. I. Kogan, JETP Lett. **37** (1983) 730; B. L. Ioffe and A. G. Oganesian, Phys. Rev. D **57** (1998) R6590.
- [14] T. Nishikawa, S. Saito and Y. Kondo, Phys. Rev. Lett. **84** (2000) 2326.
- [15] B. L. Ioffe, Nucl. Phys. **B188** (1981) 317.
- [16] L.J. Reinders, H. Rubinstein and S. Yazaki, Phys. Rep. **127** (1985) 1.
- [17] H. Kim, Phys. Rev. C **61** (2000) 019801.
- [18] H. Kim, nucl-th/9906081, Prog. Theo. Phys. **103** (2000) 1001.
- [19] D.B. Leinweber, Phys. Rev. D **51** (1995) 6383.
- [20] P. G. Ratcliffe, Phys. Lett. B **365** (1996) 383.; hep-ph/9710458.
- [21] D. K. Griegel, Ph.D thesis, University of Maryland (1991).

FIGURES

FIG. 1. The Borel curve for the πNN coupling from the $i\gamma_5$ structure. $g_{\pi N}\lambda_N^2(t)$ is determined by taking the intersection of the vertical axis ($M^2 = 0$) with the best-fitting linear curve. (See also Section V). The thick lines are for $S_0 = 2.07 \text{ GeV}^2$ while the thin lines are for $S_0 = 2.57 \text{ GeV}^2$. The three different sets of curves correspond to three different values of t . The long-dashed lines are for $t = 1.5$, the solid lines for $t = -1.5$ and the dot-dashed lines for $t = -1.0$. The difference by changing the continuum threshold is only 2 – 3% at $M^2 = 1 \text{ GeV}^2$ for each t .

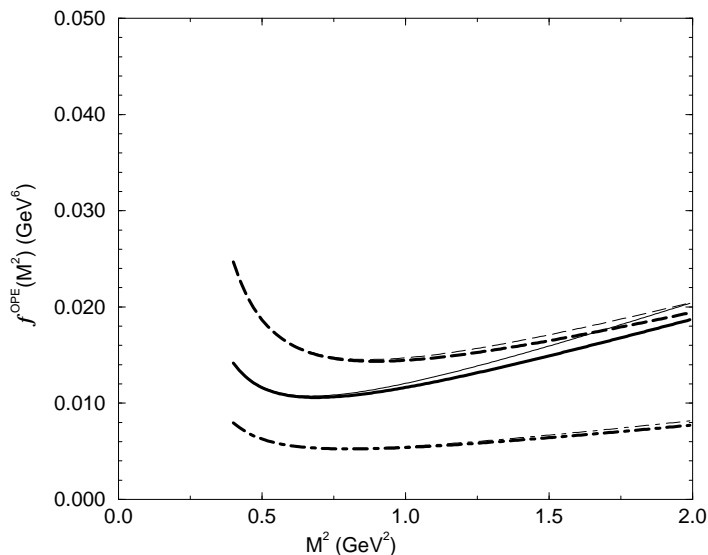


FIG. 2. The Borel curve for the πNN coupling from the $\gamma_5 \sigma_{\mu\nu} q^\mu p^\nu$ structure. The thick lines are for $S_0 = 2.07 \text{ GeV}^2$ case, while thin lines are for $S_0 = 2.57 \text{ GeV}^2$ case. The long-dashed, solid, or dot-dashed lines correspond to $t = 1.5, -1.5, -1.0$, respectively. The difference by changing the continuum threshold is only 2 – 3% level at $M^2 = 1 \text{ GeV}^2$ for each t .

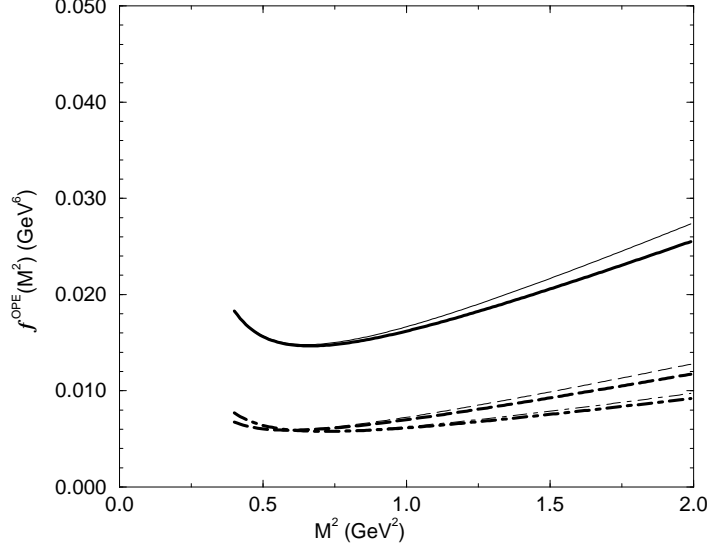


FIG. 3. The Borel curve for the πNN coupling from the $i\gamma_5 \not{p}$ structure. Each curve is obtained similarly as the $i\gamma_5$ and $\gamma_5 \sigma_{\mu\nu} q^\mu p^\nu$ cases. The difference by changing the continuum threshold is large, almost 15% level at $M^2 = 1 \text{ GeV}^2$.

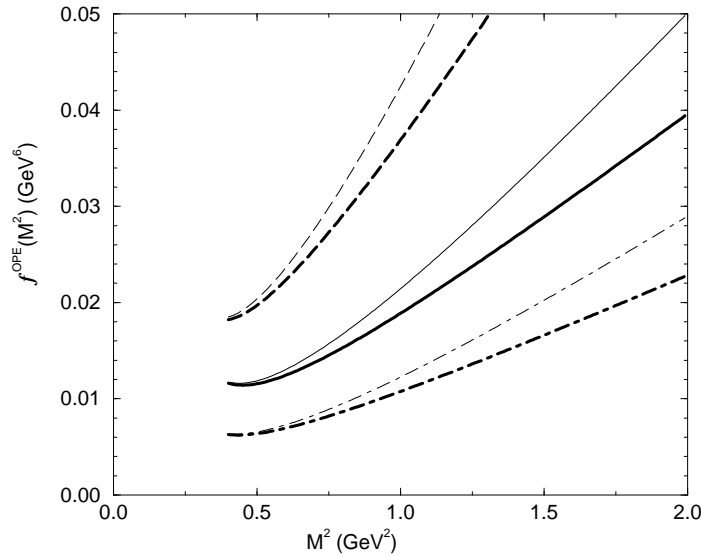


FIG. 4. $[g_{MB}\lambda_B^2(t)]_{\text{fitted}}$ from the $i\gamma_5$ structure is plotted as a function of t , for πNN , ηNN , $\pi\Sigma\Sigma$, $\eta\Sigma\Sigma$, $\pi\xi\xi$, $\eta\xi\xi$. We choose the Borel window as $0.65 \leq M^2 \leq 1.24 \text{ GeV}^2$, and the continuum threshold as $S_0 = 2.07 \text{ GeV}^2$.

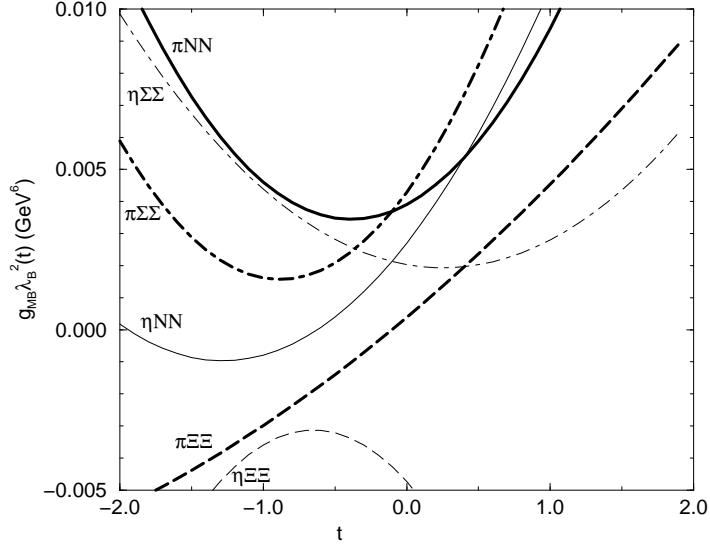


FIG. 5. $[g_{MB}\lambda_B^2(t)]_{\text{fitted}}$ from the $\gamma_5\sigma_{\mu\nu}q^\mu p^\nu$ structure is plotted as a function of t .

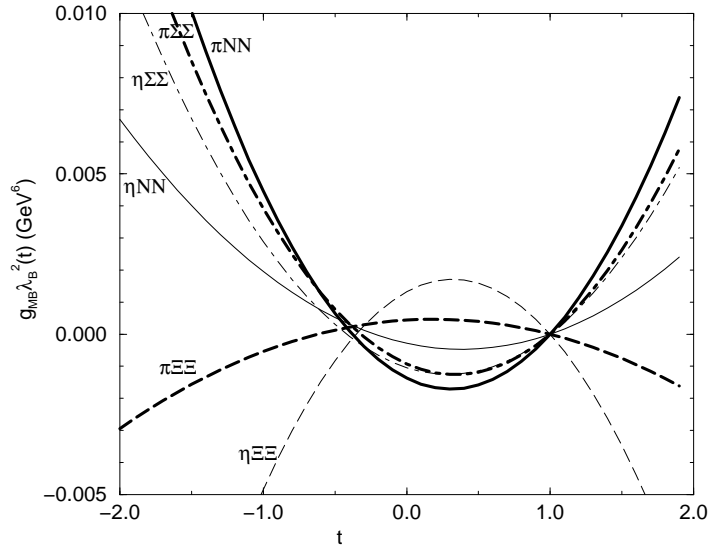


FIG. 6. $\lambda_B^2(t)$ is plotted with the thick solid line as a function of t using chiral-odd nucleon mass sum rule Eq. (23) at $M^2 = 1 \text{ GeV}^2$ and the continuum threshold $S_0 = 2.07 \text{ GeV}^2$. Also shown with the thin long-dashed line (the thin dot-dashed line) is for $M^2 = 1.2 \text{ GeV}^2$, $S_0 = 2.07 \text{ GeV}^2$ ($M^2 = 1 \text{ GeV}^2$, $S_0 = 2.57 \text{ GeV}^2$).

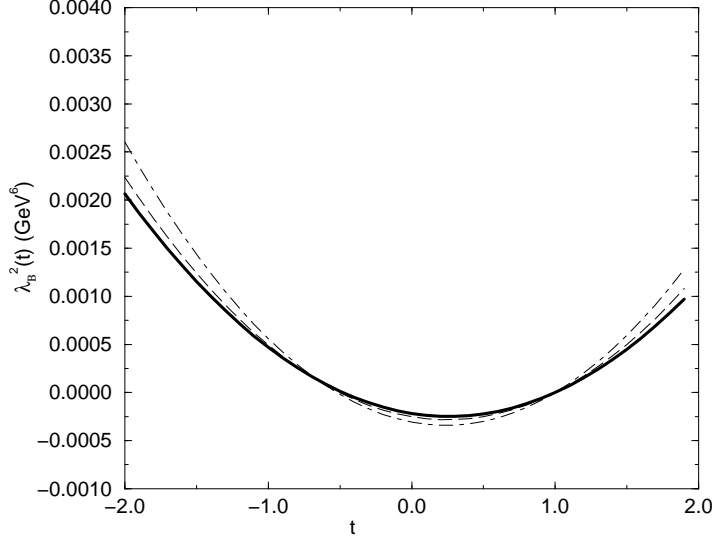


FIG. 7. The F/D ratio from the $\gamma_5 \sigma_{\mu\nu} q^\mu p^\nu$ structure is plotted as a function of $\cos \theta$, where θ is defined as $\tan \theta = t$. (See the text.) Corresponding t is also shown at the top of the figure. Circles are obtained with $0.65 \leq M^2 \leq 1.24 \text{ GeV}^2$ and the continuum threshold $S_0 = 2.07 \text{ GeV}^2$, triangles ; $0.65 \leq M^2 \leq 1.24 \text{ GeV}^2$, $S_0 = 2.57 \text{ GeV}^2$, squares ; $0.90 \leq M^2 \leq 1.50 \text{ GeV}^2$, $S_0 = 2.07 \text{ GeV}^2$. In the realistic region $-0.78 \lesssim \cos \theta \lesssim 0.61$, the F/D ratio is insensitive to t .

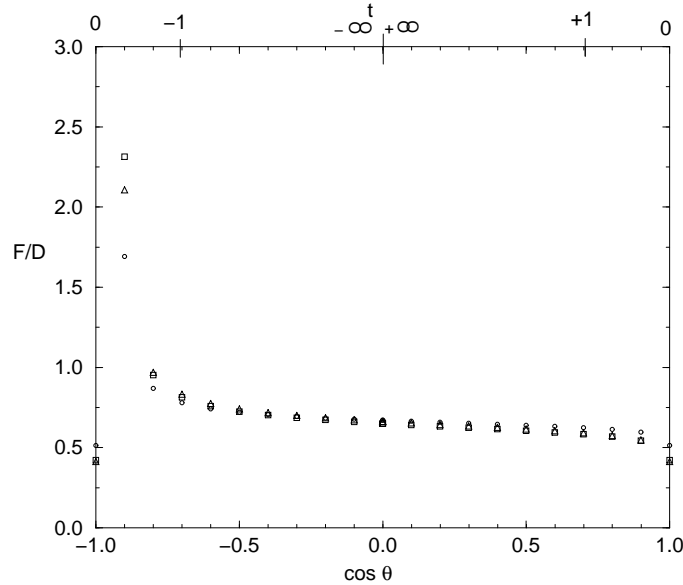


FIG. 8. The F/D ratio from the $i\gamma_5$ structure is plotted as a function of $\cos \theta$. See the caption of Fig. 7 for the explanation of each symbol. The F/D ratio is sensitive to t and we can not predict reliable value.

